Eur. Phys. J. D **38**, 315–322 (2006)
DOI: 10.1140/epjd/e2006-00032-4

THE EUROPEAN PHYSICAL JOURNAL D

Loss estimation of electrostatically trapped ND_3 molecules

M. Kajita[a]

National Institute of Information and Communications Technology, 4-2-1 Nukui-Kitamachi, Koganei, Tokyo 184-8795, Japan

Received 28 September 2005 / Received in final form 21 December 2005
Published online 8 February 2006 –

Abstract. Losses of electrostatically trapped molecules are caused by the Majorana transition or the inelastic collisions between trapped molecules. The loss rate of electrostatically trapped ND_3 molecules in the $(J = 1, K = 1, M = 1, \mathrm{A})$ state was estimated: ND_3 molecules in this state have actually been trapped. When trapping cold molecules, using $^{15}ND_3$ molecules (fermion) with a minimum electric field higher than 10 kV/cm yields high stability.

PACS. 34.10.+x General theories and models of atomic and molecular collisions and interactions (including statistical theories, transition state, stochastic and trajectory models, etc.) – 34.50.Ez Rotational and vibrational energy transfer

1 Introduction

Studying cold polar molecules is worthwhile, because the dipole-dipole interaction is not spherically symmetric and works at a long distance range. Baranov et al. and Goral et al. theoretically analyzed the Bose-Einstein condensation (BEC) and Fermi degeneracy of trapped polar molecules [1–4]. DeMille proposed to use trapped polar molecules for a quantum computers [5]. Three ways of trapping cold molecules have been developed: pairing ultracold atoms in an optical or magnetic trap, cooling of molecules by colliding them with cold gas, and obtaining a slow molecular beam using deceleration or selecting of slow molecules.

The first method uses photoassociation or Feshbach resonance. Kerman et al. produced ultracold RbCs* molecules using photoassociation [6]. Inouye et al. [7] and Stan et al. [8] produced cold KRb and LiNa molecules using Feshbach resonance. However, molecules constructed using photoassociation or Feshbach resonance are mostly in excited states. Sage et al. obtained cold RbCs molecules in the absolute ground state [9], using the method proposed by Kerman et al. [10]. However, the number of molecules in the ground state was very low.

The second method has been developed since 1997. Using a static magnetic field, Harvard group trapped CaH molecules precooled through buffer-gas collision [11,12]. This method is useful only for paramagnetic molecules. Using an electrostatic trap is preferable for non-paramagnetic molecules. However, using buffer-gas cooling to load molecules into an electrostatic trap with high voltage is difficult, because of the break down between the electrodes. There is also an idea to cool trapped molecules (with the methods shown below) through the collision with laser cooled atoms [13].

For the third method, the possibilities of molecular laser cooling have been discussed by several groups. Bahns et al. generally discussed laser cooling using a multiple single frequency laser [14]. The possibility of Doppler cooling of CaH molecular beam was discussed by di Rosa [15]. Novel cooling systems using optical cavities were proposed by Horal et al. [16] and Vuletic et al. [17]. However, molecules have never actually been laser cooled.

Several other methods have been developed to get slow molecular beams. A deceleration method using a time-varying electric field has been developed to load polar molecules into a trap electrode [18–20]. Bethlem et al. and Crompvoets et al. have loaded decelerated molecules into the space enclosed by the quadrupole electrodes [21] and the ring electrodes [22], respectively. Junglen et al. have constructed a quadrupole guide for selecting slow molecules from a continuous molecular beam [23]. Molecules selected by this quadrupole guide were loaded into a electric trap [24]. A counter-rotating beam source [25,26] or the billiard-like collisions in crossed beams [27] can also be used to get slow molecules.

Note that the trapping experiments by Bethlem et al. and Crompvoets et al. and have succeeded mainly with ND_3 molecules in the $(J = 1, K = 1, M_J = \pm 1, \mathrm{A})$ state (weak-field seeking state). Here, J denotes the quantum numbers of the total rotational angular momentum, K and M_J are the quantum numbers of the trajectory of the molecular rotational angular momentum parallel to the molecular axis and electric field, and A is the anti-symmetric state. Recently also ND_3 molecules in the

[a] e-mail: kajita@nict.go.jp

($J = 1, K = 1, M_J = \pm 1$, S) state (strong-field seeking state) have been trapped using AC electric field [28]. Here, S denotes the symmetric states. The experiments by Junglen et al. and Rieger et al. were first performed using ND_3 molecules; they later also succeeded using CH_2O and CH_3Cl molecules [23,24]. ND_3 molecules can easily be electrostatically manipulated for the following reasons: (1) the Stark effect is significant because of the molecule's large permanent dipole moment and narrow inversion doublet (1.6 GHz for $^{14}ND_3$ and 1.4 GHz for $^{15}ND_3$); (2) the maximum trap depth in a DC-electric field is large, because of the molecule's large rotational constant B (= 154 GHz); (3) when ND_3 molecules are seeded into a Xe supersonic beam, the initial kinetic energy (before the electric deceleration) of the molecules is reduced because of the small value of (mass[ND_3]/mass[Xe]); (The velocity distribution becomes uniform inside a supersonic beam.) (4) the populations in the weak-field seeking states are rather large because $J = K = 1$ is the ground state of para-ammonia molecules. OH molecules also have the advantages listed above. Bochinski et al. decelerated an OH molecular beam first [29,30], and van de Meerakker et al. electrostatically trapped OH molecules [31].

Evaporative cooling is a useful method of reducing the temperature of trapped molecules, which is possible when the trap loss rate is much less than the elastic collision rate [32,33]. Although trap loss is also caused by technical losses, such as collisions with background gas and noise in the trap potential, we discuss only the intrinsic loss caused by the transition from the weak- to strong-field seeking states. These transitions are caused by the Majorana effect (the transition between quantum states caused by a change in the electric-field direction) or inelastic collisions. The Majorana transition of electrostatically trapped linear polar molecules has been analyzed in reference [34]. It was shown that the Majorana transition rate is inversely proportional to the energy gaps between different sub-levels. The elastic and inelastic collisions between electrostatically trapped linear polar molecules in the $^1\Sigma$ state have been discussed in references [35–39] and those in the $^2\Pi$ state have been discussed in references [40–42]. When the collisional kinetic energy E is high enough to be treated semi-classically ($E > 1$ K), the elastic collision cross-section decreases $(\propto E^{-1/2})$ and the inelastic collision cross-section becomes maximum at a certain value of E (depends on the change of total internal energy) [35,38]. When E is low enough to use the Born approximation ($E < 10^{-5}$ K), the elastic collision cross-section is constant at any value of E and the inelastic collision cross-section is proportional to $E^{-1/2}$ for boson and $E^{1/2}$ for fermion isotopes, respectively [37,39,41]. At ultra-low temperatures, fermion isotopes can be trapped with higher stability than boson isotopes because of their lower collision loss rate. The dependence of the collision cross-sections on the electric field is rather complicated because of the coupling of different states. The inelastic collision cross-section is reduced significantly, taking on a special electric field value where different states have a level crossing between them [39].

We estimated the loss rate of ND_3 molecules in the ($J = 1, K = 1, M_J = 1$, A) state trapped by a DC electric field. Trap loss is caused by transitions to the ($J = 1$, $K = 1$, $M_J = 1$, S) state or the ($J = 1, K = 1, M_J = 0$, A or S) states. ND_3 is a symmetric-top molecule, and the dependence of its trap loss rates on the electric field is quite different from that of linear molecules.

2 Stark energy shift of ND_3 molecule in the ($J = 1$, $K = 1$) state

The energy structures of ND_3 molecules are given by $(J, K, I_D, F_1, F, M_F, \Omega)$ ($\Omega, \Omega' =$ A or S) in the field free space, where I_D is the nuclear spin of D atoms (1 or 2 for $K = 1$) and M_F is the quantum number of the component of the hyperfine angular momentum parallel to the electric field. F_1 and F are given as follows using I_N $\left(= 1 \text{ for } ^{14}\text{N and } 1/2 \text{ for } ^{15}\text{N}\right)$ as the nuclear spin of an N atom

$$F_1 = J + I_N, \qquad F = F_1 + I_D.$$

Van Veldhoven et al. precisely measured hyperfine structures of $^{14}ND_3$ and $^{15}ND_3$ isotopes [43,44]. When the electric field is so high that the interaction between the electric dipole moment and electric field is much stronger than the hyperfine interaction, M_J (the parameter that determines the Stark effect) must be more deterministic than F_1 and F. Therefore, the energy structure under the high electric field is not described by the hyperfine quantum numbers, but by $(J, K, I_D, M_J, M_N, M_D, \Omega)$ [45]. Here, M_N and M_D denote the components of the nuclear spins of the N and D atoms parallel to the electric field, respectively. The following relations hold strictly at any electric field strength because only one combination of (M_J, M_N, M_D) holds for $M_F = M_J + M_N + M_D$

- $^{14}ND_3$

$$(J=1,K=1,I_D=1,F_1=2,F=3,M_F=\pm3,\text{A}) = (J=1,K=1,I_D=1,M_J=\pm1,M_N=\pm1,M_D=\pm1,\text{A})$$
$$(J=1,K=1,I_D=1,F_1=2,F=3,M_F=\pm3,\text{S}) = (J=1,K=1,I_D=1,M_J=\pm1,M_N=\pm1,M_D=\pm1,\text{S})$$
$$(J=1,K=1,I_D=2,F_1=2,F=4,M_F=\pm4,\text{A}) = (J=1,K=1,I_D=2,M_J=\pm1,M_N=\pm1,M_D=\pm2,\text{A})$$
$$(J=1,K=1,I_D=2,F_1=2,F=4,M_F=\pm4,\text{S}) = (J=1,K=1,I_D=2,M_J=\pm1,M_N=\pm1,M_D=\pm2,\text{S})$$

- $^{15}ND_3$

$$(J=1,K=1,I_D=1,F_1=\frac{3}{2},F=\frac{5}{2},M_F=\pm\frac{5}{2},\text{A}) = (J=1,K=1,I_D=1,M_J=\pm1,M_N=\pm\frac{1}{2},M_D=\pm1,\text{A})$$

$$(J=1,K=1,I_D=1,F_1=\frac{3}{2},F=\frac{5}{2},M_F=\pm\frac{5}{2},\mathrm{S})=(J=1,K=1,I_D=1,M_J=\pm1,M_N=\pm\frac{1}{2},M_D=\pm1,\mathrm{S})$$
$$(J=1,K=1,I_D=2,F_1=\frac{3}{2},F=\frac{7}{2},M_F=\pm\frac{7}{2},\mathrm{A})=(J=1,K=1,I_D=2,M_J=\pm1,M_N=\pm\frac{1}{2},M_D=\pm2,\mathrm{A})$$
$$(J=1,K=1,I_D=2,F_1=\frac{3}{2},F=\frac{7}{2},M_F=\pm\frac{7}{2},\mathrm{S})=(J=1,K=1,I_D=2,M_J=\pm1,M_N=\pm\frac{1}{2},M_D=\pm2,\mathrm{S}).$$

Other $(J,K,I_D,F_1,F,M_F,\Omega)$ states converge to the $(J,K,I_D,M_J,M_N,M_D,\Omega)$ states when the electric field becomes so high that $(d\epsilon)^2/\Delta_i \gg \Delta_{hf}$ is satisfied [45]. Here, d is the molecular permanent dipole moment, ϵ is the electric field strength, Δ_i is the inversion splitting, and Δ_{hf} is the hyperfine splitting. The hyperfine states, which have no significant Stark effect, converge to the $M_J=0$ states as the electric field strength increases [43,44]. The hyperfine states $(J,K,I_D,F_1,F,M_F,\Omega)$, which converge to the $M_J=0$ states, are shown below

- $^{14}ND_3$

$$(J=1,K=1,I_D=1,F_1=2,F=2,|M_F|\le2,\mathrm{A})\rightarrow(J=1,K=1,I_D=1,M_J=0,M_N,M_D,\mathrm{A})$$
$$(J=1,K=1,I_D=1,F_1=1,F=2,|M_F|\le2,\mathrm{S})\rightarrow(J=1,K=1,I_D=1,M_J=0,M_N,M_D,\mathrm{S})$$
$$(J=1,K=1,I_D=2,F_1=2,F=4,|M_F|\le3,\mathrm{A})\rightarrow(J=1,K=1,I_D=2,M_J=0,M_N,M_D,\mathrm{A})$$
$$(J=1,K=1,I_D=2,F_1=1,F=3,|M_F|\le3,\mathrm{S})\rightarrow(J=1,K=1,I_D=2,M_J=0,M_N,M_D,\mathrm{S})$$

$$M_F=M_N+M_D,\qquad M_N=\pm1,0,\qquad M_D=\pm1,0$$

- $^{15}ND_3$

$$(J=1,K=1,I_D=1,F_1=\frac{3}{2},F=\frac{3}{2},|M_F|\le\frac{3}{2},\mathrm{A})\rightarrow(J=1,K=1,I_D=1,M_J=0,M_N,M_D,\mathrm{A})$$
$$(J=1,K=1,I_D=1,F_1=\frac{3}{2},F=\frac{3}{2},|M_F|\le\frac{3}{2},\mathrm{S})\rightarrow(J=1,K=1,I_D=1,M_J=0,M_N,M_D,\mathrm{S})$$
$$(J=1,K=1,I_D=2,F_1=\frac{3}{2},F=\frac{7}{2},|M_F|\le\frac{5}{2},\mathrm{A})\rightarrow(J=1,K=1,I_D=2,M_J=0,M_N,M_D,\mathrm{A})$$
$$(J=1,K=1,I_D=2,F_1=\frac{1}{2},F=\frac{5}{2},|M_F|\le\frac{5}{2},\mathrm{S})\rightarrow(J=1,K=1,I_D=2,M_J=0,M_N,M_D,\mathrm{S})$$

$$M_F=M_N+M_D,\qquad M_N=\pm\frac{1}{2},\qquad M_D=\pm1,0.$$

Other hyperfine states have significant Stark effects, and they converge to the $M_J=\pm1$ states as the electric field strength increases [43,44]. The hyperfine splittings are less than 1.6 MHz for the $^{14}ND_3$ and 0.3 MHz for the $^{15}ND_3$ isotopes, respectively [43,44]. The value of d is 1.48 D and $(d\epsilon)^2/\Delta_i \gg \Delta_{hf}$ is satisfied when $\epsilon \gg 0.1$ kV/cm (for $^{15}ND_3$ 0.02 kV/cm). We discuss only the case when $\epsilon \gg 0.1$ kV/cm. The nuclear spins (M_N, M_D) do not influence the Stark energy shift and the dipole matrix elements. Therefore, we describe the quantum states by only (J,K,M_J,Ω).

Figure 1 shows the energy levels of ND_3 molecules in the $(J=1,K=1)$ states as a function of the electric field, which was calculated taking the coupling of the $J=1-3$ states into account. Because of the small splitting between the inversion levels and the large rotational constant, B, the Stark energy shifts of the $M_J=\pm1$ states are proportional to ϵ with 2 kV/cm $< \epsilon <$ 100 kV/cm. An electric trap can easily be made with a trap potential depth larger than 1 K. The ($M_J=0$, A or S) states have slightly negative Stark energy shifts, induced by the coupling with the ($J\ge2$, $K=1$) states. Molecules in the $M_J=0$ states cannot be trapped by a DC electric field and trapping using an AC electric field also seem difficult because the Stark energy shift is very small (< 0.1 K at $\epsilon = 100$ kV/cm).

3 Majorana transition

The Majorana effect is the M-changing transition caused by the change of the electric field direction. For the trapped molecules, the Majorana transition can be caused by the molecular motion inside the electric trap. The Majorana effect can cause a ($J=1, K=1, M_J=\pm1$, A) $\rightarrow$ ($J=1$, $K=1$, $M_J=0$, A) transition. Because the $M_J=0$ states are strong-field seeking states, this transition causes the trap loss.

When molecules are trapped due to the linear Stark effect (depending on the sign of the electric field), Majorana loss is caused when the sign of the electric field flips. However, the Stark effect of the ND_3 molecules does not depend on the sign of the electric field, but only on the angle between the directions of electric field and the molecular axis (parallel or perpendicular). Therefore, we analyzed the Majorana loss of an ND_3 molecule using a model, in

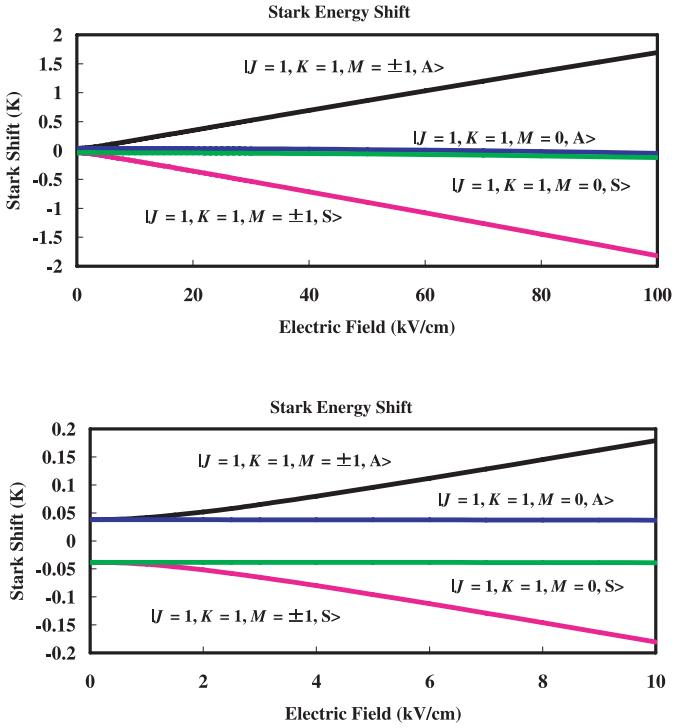

Fig. 1. Energy levels of ND_3 molecules in the $(J = 1, K = 1)$ states as a function of the electric field.

which the direction of the electric field at the molecule rotates in the xz-plane ($\vec{\epsilon} = \epsilon_0 (\sin\omega_0 t, 0, \cos\omega_0 t)$) as shown in reference [34]. The Schrödinger equation for the rotational wavefunction is given by

$$i\hbar\frac{\partial}{\partial t}\Psi = H\Psi, \qquad H = H_0 - \vec{d}\cdot\vec{\epsilon} \tag{1}$$

where H_0 is the Hamiltonian concerning the molecular rotational-inversion energy and $\vec{d}$ is the dipole moment operator. In the $x'y'z'$-frame rotating with the electric field, (1) is transformed into

$$\begin{aligned} i\hbar\frac{\partial}{\partial t}\Psi' &= (H' + V)\,\Psi' \\ \Psi' &= e^{-i\omega_0 t\widehat{J}_y}\Psi = \sum_{M_J} a\,(M_J)\,|J, M_J\rangle \\ H' &= e^{-i\omega_0 t\widehat{J}_y} H e^{i\omega_0 t\widehat{J}_y} = H_0 - d_{z'}\epsilon_0 \\ V &= \hbar\omega_0\widehat{J}_y \end{aligned} \tag{2}$$

where $\widehat{J}$ is the angular momentum operator. We assume that $J = 1$ and $M_J = 0, \pm 1$. Taking the initial state as $M_J = 1$, the Majorana transition rate $(1/\tau)$ is approximated by

$$1/\tau = \left[-\frac{d}{dt}\left|a\,(1)\right|^2\right]_{\max} = \frac{\omega_0}{2}\sqrt{\frac{1}{1 + (\pi\delta/\omega_0)^2}} \tag{3}$$

where δ is the transition frequency between the $M_J = \pm 1$ and $M_J = 0$ states. When linear molecules (for example, NaCl) in the $(J = 1, M_J = 0)$ state are trapped,

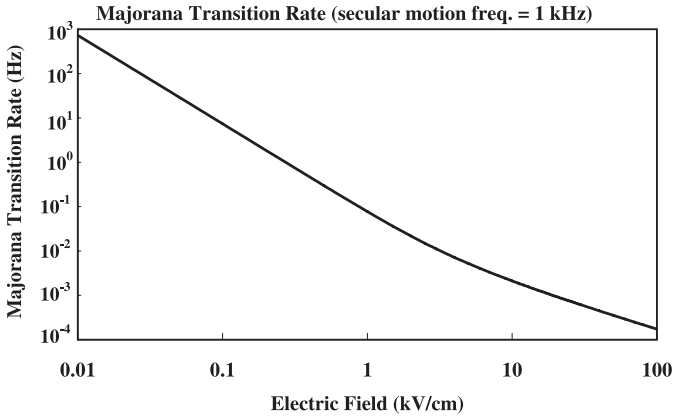

Fig. 2. Majorana transition rate of ND_3 molecules in the $(J = 1, K = 1, M_J = 1)$ as a function of electric field.

the Majorana transition rate is double the result shown in (3) [34]. This difference is due to the number of the transition channels; for ND_3 molecule one channel $(M_J = 1 \to 0)$ and for NaCl two channels $(M_J = 0 \to 1 \text{ or } -1)$.

For a trapped molecule, the change of the electric field direction is actually caused by the molecular periodic motion inside the trap. Therefore, the electric field direction also changes with the frequency of the molecular motion. We can reasonably take the angular frequency of the molecular motion in the trap area as a typical value of ω_0. Figure 2 shows $(1/\tau)$ as a function of the electric field, assuming that $\omega_0 = 2\pi \times 1$ kHz (Bethlem et al., experimentally found that $\omega_0 = 2\pi \times 0.77$ kHz [21]). With the electric field higher than 100 V/cm, $(1/\tau)$ is much less than 1 Hz.

Equation (3) is not valid when the electric field is lower than 100 V/cm, where the quantum energy state is described by the hyperfine structure. In this situation, the Majorana transition does not cause the loss of trapped molecules, except for the $^{14}ND_3$ molecules in the $(J = 1, K = 1, I_D = 2, F_1 = 2, F = 4, \text{A})$ states and the $^{15}ND_3$ molecules in the $(J = 1, K = 1, I_D = 2, F_1 = 3/2, F = 7/2, \text{A})$ and $(J = 1, K = 1, I_D = 2, F_1 = 1/2, F = 5/2, \text{A})$ states [43].

4 Intermolecular collision

4.1 Dipole matrix elements

Here we estimate the elastic and inelastic collision cross-sections of ND_3 molecules in the $(J = 1, K = 1, M_J = 1, \text{A})$ state, assuming that the collisions are caused by only the dipole-dipole interaction. The collision cross-sections are determined by the dipole matrix elements, which are obtained from

$$\langle J_{m'}, K_{m'}, M_{Jm'}, \Omega_{m'}|\vec{d}|J_m, K_m, M_{J_m}, \Omega_m\rangle = \sum_{n,n'}\beta_{m,n}\beta_{m',n'}\langle J', K', M'_J, \Omega'|\vec{d}|J, K, M_J, \Omega\rangle_0$$

$$|J_m, K_m, M_{J_m}, \Omega_m\rangle = \sum_n \beta_{m,n}\,|J_n, K_n, M_{J_n}, \Omega_n\rangle_0$$

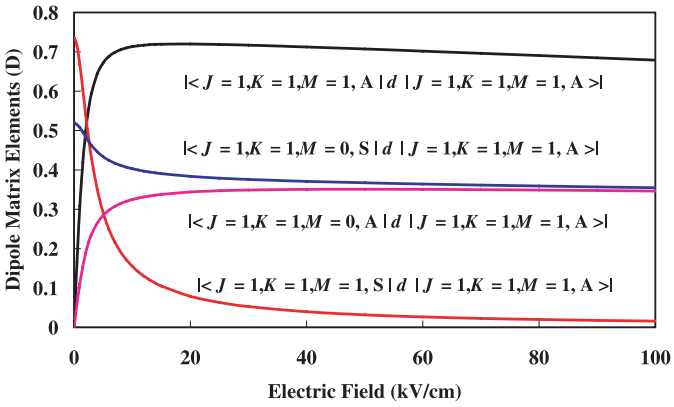

Fig. 3. Dipole matrix elements $|\langle M_J = 1, \mathrm{A}|\vec{d}|M_J = 1, \mathrm{A}\rangle|$, $|\langle M_J = 1, \mathrm{S}|\vec{d}|M_J = 1, \mathrm{A}\rangle|$, $|\langle M_J = 0, \mathrm{A}|\vec{d}|M_J = 1, \mathrm{A}\rangle|$, and $|\langle M_J = 0, \mathrm{S}|\vec{d}|M_J = 1, \mathrm{A}\rangle|$ of ND_3 molecule in the $J = K = 1$ state as a function of electric field.

where $|J_n, K_n, M_{Jn}, \Omega_n\rangle_0$ denote wavefunctions with zero-electric field and the β_n are the eigenvector components of the Hamiltonian matrix, which show the mixture of the wavefunctions. The non-zero dipole matrix elements in field free space are

$$\langle J, K, M_J, \mathrm{A}|\vec{d}|J, K, M_J, \mathrm{S}\rangle_0 = \langle J, K, M_J, \mathrm{S}|\vec{d}|J, K, M_J, \mathrm{A}\rangle_0 = \frac{KM_J}{J(J+1)}d$$

$$\langle J+1, K, M_J, \mathrm{A}|\vec{d}|J, K, M_J, \mathrm{S}\rangle_0 = \langle J+1, K, M_J, \mathrm{S}|\vec{d}|J, K, M_J, \mathrm{A}\rangle_0 = \frac{K\sqrt{(J+1)^2 - M_J^2}}{(J+1)\sqrt{(2J+1)(2J+3)}}d$$

$$\langle J-1, K, M_J, \mathrm{A}|\vec{d}|J, K, M_J, \mathrm{S}\rangle_0 = \langle J-1, K, M_J, \mathrm{S}|\vec{d}|J, K, M_J, \mathrm{A}\rangle_0 = -\frac{K\sqrt{J^2 - M_J^2}}{J\sqrt{(2J+1)(2J-1)}}d$$

which shows that the elastic collision is not caused by the dipole-dipole interactions when there is no electric field. Under an electric field, also dipole matrix elements $(\Omega, \Omega') = (\mathrm{S}, \mathrm{S})$ and (A, A) are induced, which makes elastic collisions possible. The collisional transitions to the $(J = 1, K = 1, M_J = 1, \mathrm{S})$, $(J = 1, K = 1, M_J = 0, \mathrm{A})$, and $(J = 1, K = 1, M_J = 0, \mathrm{S})$ states are possible, which cause the trap loss. The $J = 1 \rightarrow 2$ transition is significant only when the collisional kinetic energy is much larger than $4hB(\approx 30\ \mathrm{K})$. Figure 3 shows the dipole matrix elements $|\langle M_J = 1, \mathrm{A}|\vec{d}|M_J = 1, \mathrm{A}\rangle|$, $|\langle M_J = 1, \mathrm{S}\ |\vec{d}|M_J = 1, \mathrm{A}\rangle|$, $|\langle M_J = 0, \mathrm{A}|\vec{d}|M_J = 1, \mathrm{A}\rangle|$, and $|\langle M_J = 0, \mathrm{S}\ |\vec{d}|M_J = 1, \mathrm{A}\rangle|$ with $J = K = 1$ as a function of the electric field. These values were calculated taking the coupling between the $J = 1 - 3$ states into account. As the electric field, ϵ, increases, the mixture of the wavefunctions $|J = 1, K = 1, M_J = 1, \mathrm{A}\rangle$ and $|J = 1, K = 1, M_J = 1, \mathrm{S}\rangle$ becomes significant. The dipole matrix elements $|\langle M_J = 1, \mathrm{A}|\vec{d}|M_J = 1, \mathrm{A}\rangle|$ and $|\langle M_J = 0, \mathrm{A}|\vec{d}|M_J = 1, \mathrm{A}\rangle|$ are proportional to ϵ when $\epsilon < 1$ kV/cm, but they are almost constant when $\epsilon > 5$ kV/cm. The dipole matrix element $|\langle M_J = 1, \mathrm{S}|\vec{d}|M_J = 1, \mathrm{A}\rangle|$ decreases significantly as ϵ increases. The elastic collision cross-section is expected to increase rapidly as ϵ increases while $\epsilon <$1 kV/cm, but it is almost constant when $\epsilon > 5$ kV/cm.

4.2 Calculation of collision cross-sections

The cross-sections of the procedures $|\Phi_0, \Phi_0\rangle \rightarrow |\Phi_1, \Phi_2\rangle$ caused by collision between the same kind of molecules are obtained using [35,36,39–42]

$$\sigma_{(\Phi_1,\Phi_2)} = \sum_{L,M_L}\sum_{L',M'_L} \frac{4}{1+\delta(\Phi_1,\Phi_2)}\frac{\pi}{k^2} \times P\left[(\Phi_1,\Phi_2)(L,M_L) \rightarrow (L',M'_L)\right]$$

$$L, L': \begin{array}{l}\text{even numbers for bosons } (^{14}ND_3)\\ \text{odd numbers for fermions } (^{15}ND_3)\end{array} \quad (4)$$

where k is the incident wave number and L (L') and $M_L(M'_L)$ are the quantum numbers for the total angular momentum of the relative motion and its trajectory parallel to the electric field before (and after) the collision, respectively. The term P is the opacity function, given by the intermolecular interaction. Only the dipole-dipole interaction was taken into account to obtain P.

4.2.1 Ultra-low kinetic energy (Born approximation)

When the collisional interaction is weak enough, P is obtained using the first order perturbation (Born approximation). The Born approximation is valid when the collisional kinetic energy is small enough that P obtained by the first-order perturbation is much smaller than unity for each scattering terms. The dipole-dipole interaction can be simply estimated as d^2/r^3, assuming that dipole moment vectors of both molecules are exactly parallel. The above condition is actually satisfied when [42]

$$E = \frac{\hbar^2 k^2}{2m} < \frac{32}{27}\frac{16\pi^2\varepsilon_0^2\hbar^6}{m^3 d^4}. \quad (5)$$

For ND_3 molecules, (5) is satisfied when $E/k_B < 0.1\ \mu$K. However, the dipole-dipole interaction is actually much weaker than d^2/r^3, and the Born approximation is also actually valid in a region of higher kinetic energy. With more accurate calculation, $P_{\max} < 1$ is satisfied when $E/k_B < 1$ mK. In this paper, we apply the Born approximation with $E/k_B < 100\ \mu$K. Using the Born approximation, each scattering term $\pi P/k^2$ is obtained using [37]

$$\frac{\pi}{k^2}P[(\Phi_1,\Phi_2)(L,M_L) \rightarrow (L',M'_L)] = \frac{m^2}{16\pi\varepsilon_0^2\hbar^4}|\langle\Phi_1|\vec{d}|\Phi_0\rangle|^2|\langle\Phi_2|\vec{d}|\Phi_0\rangle|^2 G_{L,L'}\left(\frac{k'}{k}\right)W$$

$$G_{L,L'}\left(\frac{k'}{k}\right) = \frac{k'}{k}\left[\int_d^\infty j_L^*(kr)\,\frac{1}{r^3}\,j_{L'}(k'r)\,r^2 dr\right]^2$$
$$k = \frac{\sqrt{2mE}}{\hbar} \quad k' = \frac{\sqrt{2m(E+\Delta_E)}}{\hbar}$$
$$\Delta_E = 2R(\Phi_0) - R(\Phi_1) - R(\Phi_2) \tag{6}$$

where k' denotes the wavenumber of the scattering wave, m is the reduced mass, $R(\Phi)$ is the internal energy at the Φ state, and W is a factor determined by (Φ_1, Φ_2), (L, M_L), and (L', M'_L). Assuming $k' \gg k$,

$$G_{L,L'}\left(\frac{k'}{k}\right) \propto \left(\frac{k'}{k}\right)^{1-2L} = \left(1+\frac{\Delta_E}{E}\right)^{1/2-L} \tag{7}$$

is satisfied [46]. The elastic collision cross-section is constant with any value of the collisional kinetic energy (E). The inelastic collision cross-sections are proportional to $E^{-1/2}$ for boson molecules and $E^{1/2}$ for fermion molecules (Wigner threshold law). The result using the close-coupling method shows that (7) is actually valid in the kinetic energy area lower than 1 mK (much higher than (5)) [39,42].

The elastic and inelastic collision cross-sections were obtained using the Born approximation. The dependence collision cross-sections on the electric field (ϵ) taking $E = 10^{-7}$ K is shown in Figure 4. The inelastic collision cross-section is almost constant at any value of ϵ for $^{14}ND_3$ (boson) molecules. For $^{15}ND_3$ (fermion) molecules, the inelastic collision cross-section decreases rapidly as ϵ increases. For both isotopes, the elastic collision cross-section increases as ϵ increases while $\epsilon < 5$ kV/cm and it is almost constant when $\epsilon > 5$ kV/cm. The dependence collision cross-sections on the collisional kinetic energy (E) at $\epsilon = 1$ and 20 kV/cm is shown in Figure 5. The Wigner threshold law is actually satisfied. Figures 4 and 5 show that the inelastic collision cross-sections of $^{14}ND_3$ (boson) molecules are much larger than those of $^{15}ND_3$ (fermion) molecules. The $^{15}ND_3$ (fermion) molecules can much more easily trapped than the $^{14}ND_3$ (boson) molecules at an ultra-low temperature without collision loss. The elastic collision cross-sections of the $^{15}ND_3$ (fermion) molecules are larger than those of the $^{14}ND_3$ (boson) molecules by a factor of 3.

In this section, we have considered only the cases of collisions between molecules of the same isotopes. The cross-sections of collisions between $^{14}ND_3$ and $^{15}ND_3$ molecules are given by [37]

$$\left(^{14}ND_3 - ^{15}ND_3 \text{ cross-section}\right) = \frac{\left(^{14}ND_3 - ^{14}ND_3 \text{ cross-section}\right)}{2} + \frac{\left(^{15}ND_3 - ^{15}ND_3 \text{ cross-section}\right)}{2}. \tag{8}$$

4.2.2 Higher kinetic energy (semi-classical treatment)

When the molecules are trapped inside a ring electric trap [22], the collisions with high kinetic energy (>1 K

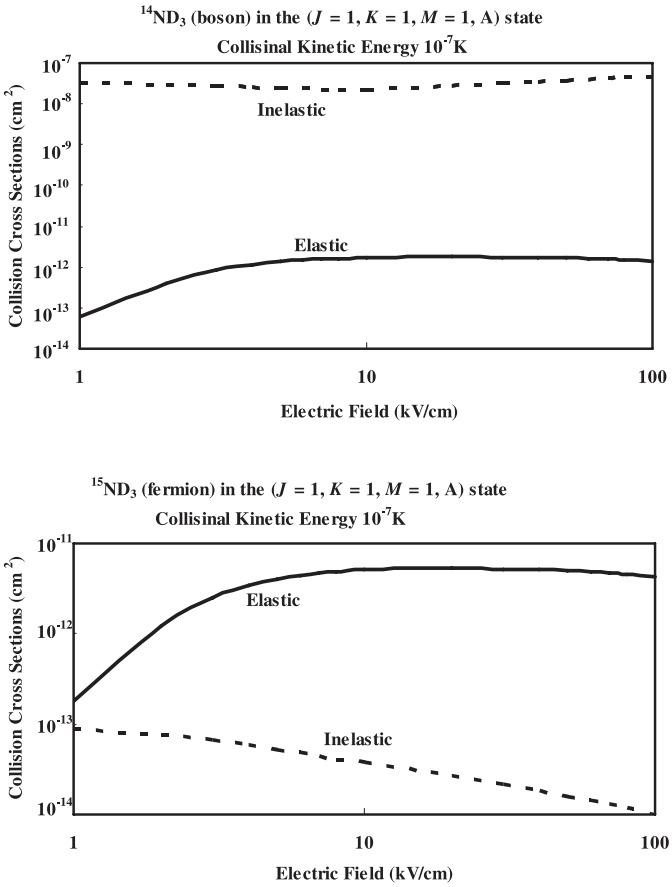

Fig. 4. Elastic and inelastic collision cross-sections of $^{14}ND_3$ and $^{15}ND_3$ molecules in the $(J = 1, K = 1, M_J = 1,$ A) state as a function of the electric field. Here the collisional kinetic energy is 10^{-7} K. Results shown in this figure were calculated using the Born approximation.

are significant. The Born approximation is not valid for such high kinetic energy. Although the close-coupling method [39–42] is in principle valid for all areas of the collisional kinetic energy (E), actually calculating it is not realistic when many partial waves must be taken into account. However, a semi-classical treatment is useful for rough estimations when E is so high that the broadening of the molecular wavepacket is much smaller than the scale size of the intermolecular interaction. Note that there is no difference between collision cross-sections of boson and fermion isotopes when many partial waves contribute to a collision. Using the impact parameter $b\,(= L/k)$, (4) is rewritten as [35,38]

$$\sigma_{(\Phi_1,\Phi_2)} = \int 2\pi b P[(\Phi_1,\Phi_2), b]\,db$$
$$P = \min(1, Q(b))$$
$$Q(b) = \frac{4}{9\hbar^2 v^2 b^4}|\langle\Phi_1|\vec{d}|\Phi_0\rangle|^2|\langle\Phi_2|\vec{d}|\Phi_0\rangle|^2 \times \exp[-\frac{1}{3}(\frac{4\Delta_E}{\pi\hbar v}b)^2]$$
$$v = \sqrt{2E/m}. \tag{9}$$

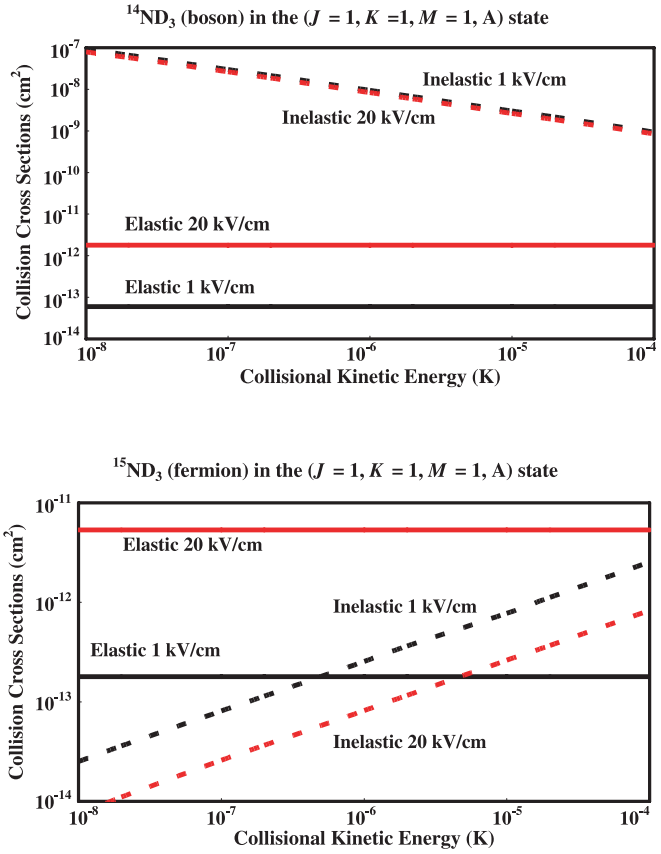

Fig. 5. Elastic and inelastic collision cross-sections of $^{14}ND_3$ and $^{15}ND_3$ molecules in the $(J = 1, K = 1, M_J = 1,$ A) state as a function of the collisional kinetic energy taking the electric field 1 and 20 kV/cm. Results shown in this figure were calculated using the Born approximation.

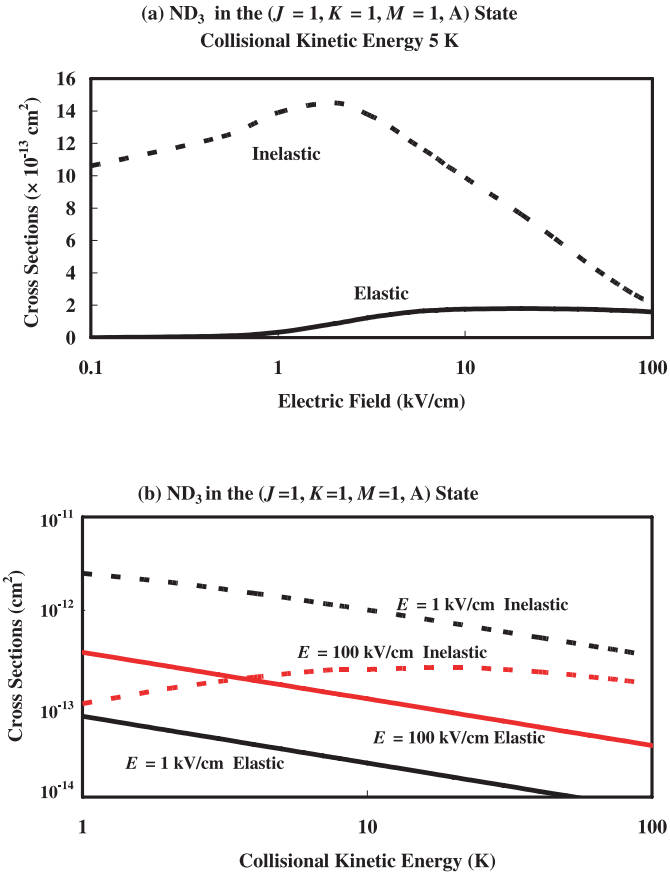

Fig. 6. Elastic and inelastic collision cross-sections of ND_3 molecule in the $(J = 1, K = 1, M_J = 1,$ A) state as functions of (a) the electric field and (b) the collisional kinetic energy. Results shown in this figure were calculated using semi-classical treatment.

Elastic and inelastic collisions as functions of the electric field and collisional kinetic energy are shown in Figure 6. The dependence of the elastic collision cross-section on the electric field (ϵ) is same as shown in Figure 4: it increases as ϵ increases when $\epsilon < 5$ kV/cm but is almost constant when $\epsilon > 5$ kV/cm. The inelastic collision cross-section reaches its maximum at $\epsilon \approx 2$ kV/cm. This is because $|\langle M_J = 0, \mathrm{A}|\vec{d}|M_J = 1, \mathrm{A}\rangle|$ increases as ϵ increases, but it becomes almost constant when $\epsilon > 2$ kV/cm. The inelastic collision cross-section decreases as ϵ increases when $\epsilon > 2$ kV/cm because the energy difference between $|M_J = 1, \mathrm{A}\rangle$ and $|M_J = 0, \mathrm{A}$ and $\mathrm{S}\rangle$ increases. The collision cross-sections are proportional to $E^{-1/2}$ when $E_0(\Delta_E) \ll E$, where E_0 is a parameter given by [38]

$$E_0(\Delta_E) = \frac{2^{7/3}m}{\hbar^2}\left[\frac{\Delta_E^2|\langle\Phi_1|\vec{d}|\Phi_0\rangle||\langle\Phi_2|\vec{d}|\Phi_0\rangle|}{\pi^2}\right]^{2/3}. \quad (10)$$

This condition is satisfied for elastic collisions and for inelastic collisions under a low electric field. When the electric field is so high that $E_0(\Delta_E) \gg E$, the inelastic collision cross-section is proportional to E. The inelastic collision cross-section is larger than the elastic collision cross-section when $E > 3$ K also giving $\epsilon = 100$ kV/cm ($E_0/k_B \approx 20$ K).

The classical path method is based on the assumption that the kinetic energy is so high that the broadening of the wavepacket is negligibly small. In the intermediate kinetic energy region (0.1–100 mK), the collision must be analyzed using the close-coupling method [39–42] taking several partial waves into account. Calculations using close-coupled method for linear molecules (OH, OD, ClCN) show that the elastic and inelastic collision cross-sections are proportional to E^{-1} with 1 mK $< E <$ 100 mK. This is because P of the scattering terms of $L = 0, 1$ saturates at value close to 1, while the contributions of other partialwaves are small.

5 Conclusion

The loss rate of ND_3 molecules trapped by a DC electric field, was estimated in consideration of the Majorana transition and the inelastic collisions. This estimation is useful, particularly because the ND_3 molecules have already been trapped [21,22,24,28]. Evaporative cooling is very difficult for ^{14} ND_3 (boson) because the collision loss rate is much higher than the elastic collision rate at any

values of the kinetic energy and electric field strength. The trapping time is shorter than 1 s when the density of $^{14}ND_3$ molecules is higher than $10^7/cm^3$ with $E/k_B = 0.1$ μK. For $^{15}ND_3$ (fermion) molecules, evaporative cooling is possible when the kinetic energy is low (<1 μK) and the electric field is high (>10 kV/cm). The trapping time is longer than 1 s when the density of $^{15}ND_3$ molecules is lower than $10^{13}/cm^3$ at $E/k_B = 0.1$ μK and $\epsilon = 10$ kV/cm. The Majorana transition rate decreases as the electric field increases. Therefore, a non-zero minimum electric field should be given at the trap center, giving an AC electric field in one direction [35]. When the kinetic energy is higher than 100 μK, evaporative cooling of $^{15}ND_3$ (fermion) molecules is also difficult. When $E/k_B = 5$ K, the trapping period is 1 s at a molecular density of $3 \times 10^8/$ cm^3.

To perform evaporative cooling, it is preferable to trap ND_3 molecules in the ($J = 1$, $K = 1$, $M_J = 1$, S) state using an AC electric field [28]. In this case, the inelastic collisions are not possible when the Stark energy shift is larger than the kinetic energy. The elastic collision rate of ND_3 molecules in the ($J = 1$, $K = 1, M_J = 1$, S) state is on the same order as that of those in the ($J = 1$, $K = 1, M_J = 1$, A) state, while the frequency of the AC electric field is much less than Δ_i. Considering just the intrinsic loss (Majorana loss), the trapping period is longer than 100 s when the electric field is higher than 10 kV/cm. The trapping period is actually determined by the technical loss, for example collision with back ground gas.

We are thankful to Prof. H. Odashima (Meiji U., Japan) for the discussion about the Majorana transition.

References

1. L. Santos, G.V. Shlyapnikov, M. Lewenstein, Phys. Rev. Lett. **90**, 250403 (2003)
2. M.A. Baranov, M.S. Mar'enko, V.S. Rychkov, G.V. Shlyapnikov, Phys. Rev. A **66**, 13606 (2002)
3. M.A. Baranov, L. Dobrek, M. Lewenstein, Phys. Rev. Lett. **92**, 250403 (2004)
4. K. Goral, B.G. Englert, K. Rzazewski, Phys. Rev. A **63**, 033606 (2001)
5. D. DeMille, Phys. Rev. Lett. **88**, 067901 (2002)
6. A.J. Kerman, J.M. Sage, S. Sainis, T. Bergeman, D. DeMille, Phys. Rev. Lett. **92**, 033004 (2004)
7. S. Inouye, J. Goldwin, M.L. Olsen, C. Ticknor, J.L. Bohn, D.S. Jin, Phys. Rev. Lett. **93**, 183201 (2004)
8. C.A. Stan, M.W. Zwierlein, C.H. Schunck, S.M.F. Raupach, W. Ketterle, Phys. Rev. Lett. **93**, 143001 (2004)
9. J.M. Sage, S. Sainis, T. Bergeman, D. DeMille, Phys. Rev. Lett. **94**, 203004 (2005)
10. A.J. Kerman, J.M. Sage, S. Sainis, T. Bergeman, D. DeMille, Phys. Rev. Lett. **92**, 153001 (2004)
11. J.D. Weinstein, R. deCarvalho, T. Guillet, B. Friedrich, J.M. Doyle, Nature **395**, 148 (1998)
12. J.M. Doyle, B. Friedrich, Nature **401**, 749 (1999)
13. W. Shoelkopf, S.Y.T. van de Meerakker, B. Friedrich, G. Meijer, private communication
14. J.T. Bahns, W.C. Stwalley, P.L. Gould, J. Chem. Phys. **104**, 9689 (1996)
15. M.D. Di Rosa, Eur. Phys. J. D **31**, 395 (2004)
16. P. Horak, G. Hechenblaikner, K.M. Gheri, H. Stecher, H. Ritsch, Phys. Rev. Lett. **79**, 4974 (1997)
17. V. Vuletic, S. Chu, Phys. Rev. Lett. **84**, 3787 (2000)
18. H.L. Bethlem, G. Berden, G. Meijer, Phys. Rev. Lett. **83**, 1558 (1999)
19. H.L. Bethlem, G. Berden, A.J.A. van Roij, F.M.H. Crompvoets, G. Meijer, Phys. Rev. Lett. **84**, 5744 (2000)
20. H.L. Bethlem, G. Meijer, Int. Rev. Phys. Chem. **22**, 73 (2003)
21. H.L. Bethlem, G. Berden, F.M.H. Crompvoets, R.T. Jongma, A.J.A. van Roij, G. Meijer, Nature **406**, 491 (2000)
22. F.M.H. Crompvoets, H.L. Bethlem, R.T. Jongma, G. Meijer, Nature **411**, 174 (2001)
23. T. Junglen, T. Rieger, S.A. Rangwala, P.W.H. Pinkse, G. Rempe, Eur. Phys. J. D **31**, 365 (2004)
24. T. Rieger, T. Junglen, S.A. Rangwala, P.W.H. Pinkse, G. Rempe, e-print `arXiv:physics/0505039`
25. M. Gupta, D. Herschbach, J. Phys. Chem. A **103**, 10670 (1999)
26. M. Gupta, D. Herschbach, J. Phys. Chem. A **105**, 1626 (2001)
27. M.S. Elioff, J.J. Valentini, D.W. Chandler, Eur. Phys. J. D **31**, 385 (2004)
28. J. van Veldhoven, H.L. Bethlem, G. Meijer, Phys. Rev. Lett. **94**, 083001 (2005)
29. J.R. Bochinski, E.R. Hudson, H. Lewandowski, G. Meijer, J. Ye, Phys. Rev. Lett. **91**, 243001 (2003)
30. J.R. Bochinski, E.R. Hudson, H. Lewandowski, J. Ye, Phys. Rev. A **70**, 043410 (2004)
31. S.Y.T. van de Meerakker, P.H.M. Smeets, N. Vanhaecke, R.T. Jongma, G. Meijer, Phys. Rev. Lett. **94**, 023004 (2005)
32. W. Ketterle, N.J. van Druten, Adv. At. Mol. Opt. Phys. **37**, 181 (1996)
33. C.R. Monroe, E.A. Cornell, C.A. Sackett, C.J. Myatt, C.E. Wieman, Phys. Rev. Lett. **70**, 414 (1993)
34. M. Kajita, T. Suzuki, H. Odashima, Y. Moriwaki, M. Tachikawa, Jpn. J. Appl. Phys. **40**, L1260 (2001)
35. M. Kajita, Eur. Phys. J. D **20**, 55 (2002)
36. M. Kajita, Eur. Phys. J. D **23**, 337 (2003)
37. M. Kajita, Phys. Rev. A **69**, 012709 (2004)
38. M. Kajita, Eur. Phys. J. D **31**, 39 (2004)
39. A.V. Avdeenkov, M. Kajita, J.L. Bohn, Phys. Rev. A **73**, 022707 (2006)
40. J.L. Bohn, Phys. Rev. A **63**, 052714 (2001)
41. A.V. Avdeenkov, J.L. Bohn, Phys. Rev. A **66**, 052718 (2002)
42. A.V. Avdeenkov, J.L. Bohn, Phys. Rev. A **71**, 022706 (2005)
43. J. van Veldhoven, R.T. Jongma, B. Sartakov, W.A. Bongers, G. Meijer, Phys. Rev. A **66**, 032501 (2002)
44. J. van Veldhoven, J. Kuepper, H.L. Bethlem, B. Sartakov, A.J.A. van Roij, G. Meijer, Eur. Phys. J. D **31**, 337 (2004)
45. J.M. Jauch, Phys. Rev. **72**, 715 (1947)
46. I.S. Gradshteyn, I.M. Ryzhik, *Table of Integral, Series, and Products* (Academic Press, NY and London, 1965) p. 692